We are IntechOpen, the world's leading publisher of Open Access books Built by scientists, for scientists

6,900
Open access books available

185,000
International authors and editors

200M
Downloads

Our authors are among the

154
Countries delivered to

TOP 1%
most cited scientists

12.2%
Contributors from top 500 universities



WEB OF SCIENCE™

Selection of our books indexed in the Book Citation Index in Web of Science™ Core Collection (BKCI)

Interested in publishing with us?
Contact book.department@intechopen.com

Numbers displayed above are based on latest data collected.
For more information visit www.intechopen.com



Chapter 10

Evaluating the Integrity of Pressure Pipelines by Fracture Mechanics

Ľubomír Gajdoš and Martin Šperl

Additional information is available at the end of the chapter

http://dx.doi.org/10.5772/77358

1. Introduction

Large engineering structures made with the use of sophisticated technology often include material defects and geometrical imperfections. These defects or imperfections do not exert their influence on the initial behaviour of structures designed in accordance with standard rules. Under the action of loading varying in time, however, they can reveal themselves in long-term operation by the initiation and growth of a fatigue crack from a defect root. Similarly, stress corrosion (SC) cracks can develop in a structure when there is an initial stress concentrator and the structure is exposed to both mechanical stress and a corrosion medium. A condition for the growth of a small fatigue crack is that the level of cyclic stress should be above the limit value given by barriers existing in a steel, and a condition for the growth of SC cracks is that the stress is greater than a certain limit value for a specific corrosion medium. It is important to pay due attention to the behaviour of cracks under various gas pipeline loading conditions in different environments, and to the influence of these conditions on the residual strength and life of the gas pipeline. The existence of a crack in the wall of a high-pressure gas pipeline mostly implies a shortened remaining period of reliable operation.

2. Theoretical treatment of cracks in pipes

At the present time, the manufacturing stage of pipes for gas pipelines includes sufficient flaw detection measures, and only products free of detectable material flaws are dispatched for operation. However, there are defects that are not revealed by the required inspection, and which manifest themselves during heavy-duty operation. The most dangerous defect is the occurrence of cracks – these are due to material defects that are difficult to reveal by a standard optical inspection. If the cracks are deep, and spread to a large extent, they can pose a threat to the pipeline operation. Using fracture mechanics it is possible to evaluate

INTECH
open science | open minds

© 2012 Gajdoš and Šperl, licensee InTech. This is an open access chapter distributed under the terms of the Creative Commons Attribution License (http://creativecommons.org/licenses/by/3.0), which permits unrestricted use, distribution, and reproduction in any medium, provided the original work is properly cited.

the threat that crack-like defects can pose to the pipeline wall, depending on whether a brittle, quasi-brittle or ductile material is involved. A model description of crack-containing systems, which relies on the stress intensity factor, K, can be used for brittle and quasi-brittle fracture, and also for subcritical fatigue growth, corrosion fatigue, and stress corrosion. In these cases, the surface crack is usually located in the field of one of the membrane tensile stress components, or in the field of bending stress, or in a combination of both. The extent of the plastic zone at the crack tip is small in comparison with the dimensions of the crack and the pipeline.

If the gas pipeline is made of a high-toughness material, the plastic strains become extensive before the crack reaches instability. Hence, some elasto-plastic fracture mechanics parameter, such as the J–integral or crack opening displacement, or a two-criterion method, should be employed to assess the threat that the crack poses to the pipeline wall. Although cracks of various directions may occur in the pipe wall, we will consider here only longitudinal cracks, because they are subjected to the biggest stress (hoop stress) in the pipe wall, and they are therefore the most dangerous (when we are considering the parent metal).

2.1. Stress intensity factor for a longitudinal through crack in the pipe wall

The first theoretical solution to the problem of establishing the stress intensity factor for a long cylindrical pipe with a longitudinal through crack under internal pressure was reported by Folias (Folias, 1969) and by Erdogan with Kibler (Erdogan & Kibler, 1969). They managed to show that the problem was analogous to that of a wide plane plate with a through crack. The only adjustment needed for transition to a pipe was to introduce a correction factor to multiply the solution for the plane plate. This factor, frequently referred to as the Folias correction factor and designated by symbol M_T, is only a function of the ratio $\lambda = c/\sqrt{Rt}$, where c is the crack half-length, R is the pipe mean radius, and t is the pipe wall thickness, and thus it depends only on the geometrical parameters of the crack and the pipe (Fig. 1).

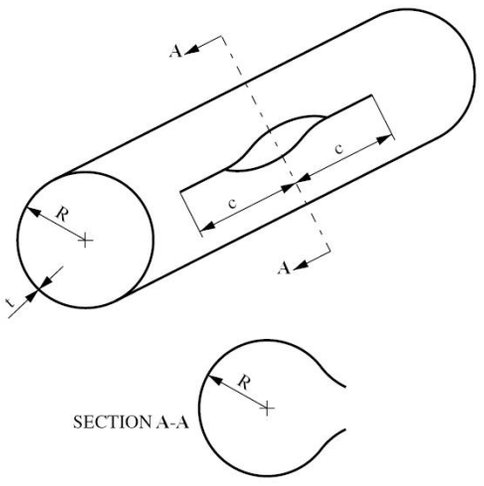


Figure 1. Deformation of a pressurized pipe in the vicinity of a longitudinal through crack

Several relations have been reported for determining the Folias correction factor. The following are the most frequently used at the present time:

The Folias relation (Folias, 1970):

$$M_T = \sqrt{1 + 1.255\lambda^2 - 0.0135\lambda^4} \tag{1}$$

The Erdogan et al. relation (Erdogan et al., 1977):

$$\begin{aligned} M_T &= 0.6 + 0.5\lambda + 0.4\exp(-1.25\lambda) \quad \text{for} \quad \omega < 5 \\ M_T &= 1.761\left(\lambda - 1.9\right)^{0.5} \quad \text{for} \quad \omega \geq 5 \end{aligned} \tag{2}$$

where $\omega = \sqrt[4]{12\left(1-\nu^2\right)}\lambda$

with ν denoting Poisson´s ratio

The following relation is the simplest:

$$M_T = \sqrt{1 + 1.61\lambda^2} \tag{3}$$

However, its validity is limited by the value λ<1.

If c is the half-length of a longitudinal through crack in the pipe, then the stress intensity factor of such a crack simply reads

$$K_I = M_T \sigma_\varphi \sqrt{\pi c} \tag{4}$$

where

$\sigma_\varphi = \pi D/2t$ is the hoop stress (D and t denoting pipe diameter and wall thickness, respectively), and

M_T is the Folias correction factor

2.2. Stress intensity factor for a longitudinal part-through crack

Various methods are used for analysing the problem of longitudinal semi-elliptical surface cracks in the wall of cylindrical shells (Fig. 2). As a 3D asymptotic solution to the stress intensity factor is virtually involved, the possibilities offered by accurate analytical procedures are confined to infinite or semi-infinite bodies. Solutions appropriate for finite bodies call for the application of approximate methods, such as the finite element method and the method of boundary integral equations, or various alternative methods (e.g. the weight function method).

The first solutions for semi-elliptical surface cracks in a plate subjected to uniaxial tension or steady bending were derived from solutions for an elliptical plane crack in an infinite 3D

body. In order to account for the finite thickness of a body and the plastic zone at the crack tip, correction factors were introduced for the "front" surface and the "rear" surface of the body and for the plastic region at the crack tip (Shah & Kobayashi, 1973). However, solutions by different authors often showed rather considerable disagreement. Scott and Thorpe (Scott & Thorpe, 1981) therefore tested the accuracy of the solutions presented by various authors by measuring changes in the shape of a crack throughout its fatigue growth. They concluded that the best engineering estimation of the stress intensity factor for a part-through crack in a plate was provided by Newman's solution (Newman, 1973). An adjusted form of this solution for a thin-walled shell is given by:

$$K_I = \left[M_F + \left(E_{(k)}\sqrt{c/a} - M_F \right) \left(\frac{a}{t} \right)^s \right] \frac{\sigma_\varphi \sqrt{\pi a}}{E_{(k)}} M_{TM} \tag{5}$$

where

M_F is the function depending on the crack geometry (on the ratio a/c)

$E_{(k)} = \int_0^{\pi/2} \sqrt{1 - k^2 \sin^2 \theta}\, d\theta$ is an elliptical integral of the second kind, k being $\sqrt{1 - \left(\frac{a}{c} \right)^2}$

s is the function depending on the crack geometry (the ratio a/c) and the relative crack depth (the ratio a/t)

$M_{TM} = \frac{\left(1 - \frac{a/t}{M_T} \right)}{\left(1 - a/t \right)}$ is the correction factor for the curvature of a cylindrical shell and for an increase in stress owing to radial strains in the vicinity of the crack root

In the last relationship, M_T is the Folias correction factor, determined by any of the relations (1) – (3). The functions M_F and s differ in form for the lowest point of the crack tip (point A in Fig. 2) and for the crack mouth on the surface of the cylindrical shell (point B in Fig. 2).

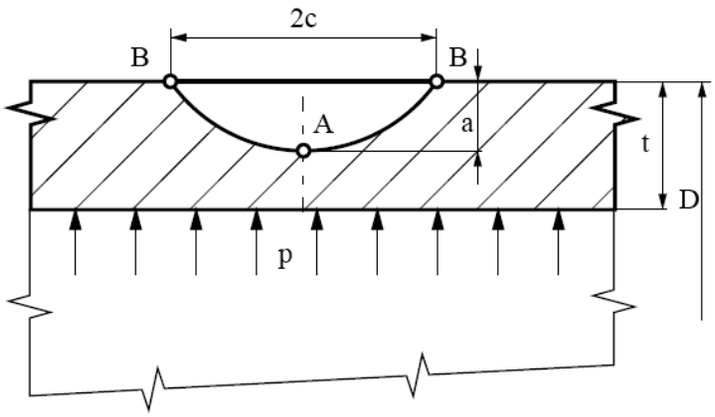


Figure 2. External longitudinal semi-elliptical crack in the wall of a cylindrical shell

2.3. Engineering methods for determining the J integral

2.3.1. The FC method

This method was proposed as the J_s method in Addendum A16 of the French nuclear code (RCC-MR, 1985). It stems from the second option for describing the transition state between ideally elastic and fully plastic behaviour of a material, i.e. from the function $f_2(L_r)$ of the R6 method (Milne et al., 1986). This function takes the form:

$$f_2\left(L_r\right)=\left(\frac{E\varepsilon_{ref}}{L_r R_e}+\frac{{L_r}^3 R_e}{2E\varepsilon_{ref}}\right)^{-1/2} \tag{6}$$

where

$L_r = \sigma/\sigma_L$ (σ – applied stress, σ_L – stress at the limit load)
R_e is the yield stress
E is Young´s modulus
ε_{ref} is the reference strain corresponding to the reference (nominal) stress σ_{ref}

If we identify function $f_2(L_r)$ with function $f_3\left(L_r\right)=\left(\frac{J}{J_e}\right)^{-\frac{1}{2}}$ and express L_r as σ_{ref} / R_e and the elastic J integral J_e as $K^2/ E´$, where E´ =E for plane stress state and E´ =$E / (1-\nu^2)$ for plane strain state, we have:

$$J=\frac{K^2}{E'}\left(\frac{E.\varepsilon_{ref}}{\sigma_{ref}}+\frac{{\sigma_{ref}}^3}{2E.{R_e}^2.\varepsilon_{ref}}\right) \tag{7}$$

The stress σ_{ref} in the above equation is a nominal stress – i.e. a stress acting in the plane where the crack occurs. Taking into consideration the description of the stress-strain dependence by the Ramberg-Osgood relation (8) and adjusting Eq. (7), we obtain the J-integral in the form (9).

$$\frac{\varepsilon}{\varepsilon_0}=\frac{\sigma}{\sigma_0}+\alpha\left(\frac{\sigma}{\sigma_0}\right)^n \tag{8}$$

$$J=\frac{K^2}{E'}\left[A+\frac{0.5\left(\sigma/\sigma_0\right)^2}{A}\right] \tag{9}$$

where

$$A=1+\alpha\left(\frac{\sigma}{\sigma_0}\right)^{n-1} \tag{10}$$

In the above equations the stress σ_0 can be substituted by the yield stress R_e ; $\varepsilon_0 = \sigma_0 / E$; α, n – material constants

As a pipeline is a body of finite dimensions, stress σ in Eqs. (9) and (10) is a nominal stress – i.e. a stress acting in the plane where the crack occurs. Referring to the R6 method (Milne et al., 1986), this stress for a pipe containing a longitudinal part-through thickness crack may be written as:

$$\sigma = \frac{\sigma_\phi}{1 - \frac{\pi a c}{2t\left(t + 2c\right)}} \tag{11}$$

In eq. (11), $\sigma_\phi = \frac{pD}{2t}$ is the hoop stress, and the meaning of the symbols *a*, *c*, and *t* is clear from Fig.2.

2.3.2. GS method

The GS method was derived by Gajdoš and Srnec (Gajdoš & Srnec, 1994) on the basis of the limit transition of the *J*-integral, formally expressed for a semi-circular notch, to a crack, with the variation of the strain energy density along the notch circumference being approximated by the third power of the cosine function of the polar angle. If the stress-strain dependence is further expressed by the Ramberg-Osgood relation (8), with $\varepsilon_0 = \sigma_0 / E$, (α, n – material constants), we can arrive at Eq. (12)

$$J = \frac{K^2}{E'}\left[1 + \frac{2\alpha n}{\left(n+1\right)}\left(\frac{\sigma}{\sigma_0}\right)^{n-1}\right] \tag{12}$$

where σ is the nominal stress in the reduced cross-section of a body. For a pipe containing a longitudinal part-through thickness crack it may be determined by relation (11).

3. Consideration of the constraint

As mentioned above, the situation existing at the crack tip in conditions of small-scale yielding can be characterized by a single fracture parameter (e.g. K, J or δ). This parameter can be used as a fracture criterion, independent of geometry. However, single-parameter fracture mechanics fails in cases of developed plasticity, where fracture toughness is a function not only of the material, but also of the dimensions and the geometry of the specimen. It is well known from the theory of fracture mechanics that for small-scale yielding the maximum stress existing at the crack tip in a non-hardening material is about $3\sigma_0$, where σ_0 is the yield stress. Single-parameter fracture mechanics apparently does not apply to non-hardening materials under fully plastic conditions, because the stress and strain fields in the vicinity of the crack tip are affected by configurations of both the body

and the crack. The situation is more favourable in hardening materials, where single-parameter fracture mechanics may approximately apply also for the developed plasticity, provided that the body maintains a high level of stress triaxiality.

The reported experimental studies suggest that the configuration of the specimen and the crack (the crack depth and the specimen dimensions, in particular) affect the fracture toughness in a brittle state. However, the fact that this configuration can also influence the R-curve of ductile materials is not so well known.

Generally, the bigger the dimension of the crack, the smaller the resistance of the material to fracture will be. The R-curve obtained on specimens with rather long cracks is, as a rule, below the R-curve obtained on specimens with rather short cracks. For this reason, standards require that the relative crack lengths be within a comparatively narrow range of values for valid values of fracture toughness J_{in}.

3.1. The J – Q theory

Some researchers dealing with fracture mechanics tried to extend the theory of fracture mechanics beyond the boundaries of the assumptions of single-parameter fracture mechanics, introducing other parameters to provide a more accurate characterization of conditions at the crack tip. One of the parameters is the so-called T-stress, which is a uniform stress acting axially (in the direction of the x-axis) in front of the crack tip in an isotropic elastic material loaded by the first mode, i.e. the opening mode, of the load. In this case, the stress field in front of the crack tip may be written as:

$$\sigma_{ij} = \frac{K_I}{\sqrt{2\pi r}} f_{ij}\left(\Theta\right) + T\delta_{1i}\delta_{1j} \tag{13}$$

The elastic T-stress heavily affects the shape of the plastic zone and the stress deep in this zone. T-stress values are linked with the stress biaxiality ratio, β, defined as

$$\beta = \frac{T\sqrt{\pi a}}{K_I} \tag{14}$$

It can be mentioned by way of illustration that the stress biaxiality ratio β equals -1 for a through crack in an infinite plate loaded by a normal stress applied far away from the crack plane. By implication, this remote stress, σ, induces a T-stress in the direction of the x-axis, whose magnitude is -σ. In an elastic case, positive values of the T-stress generally lead to a high constraint under fully elastic conditions, whereas a geometry with a negative T-stress leads to a rapid drop in the constraint as the load rises. For different geometries, the stress biaxiality ratio β can be used as a qualitative index for a relative constraint at the crack tip.

The so-called J – Q theory provides another approach to the extension of single-parameter fracture mechanics beyond the conditions of its validity. This theory aims to describe the stress field at the crack tip deep in the plastic zone. It is a well-known fact that if the small-strain theory is used, the stress field at the crack tip in the plastic zone can be described by a

power series, in which the so-called HRR solution is the leading term (Hutchinson, 1968), (Rice & Rosengren, 1968). The other terms of higher magnitudes, when summed up, provide a difference stress field, which approximately corresponds to a uniform hydrostatic shift of the stress field in front of the crack tip. It has become customary to designate the amplitude of this approximate difference stress field with letter Q, according to its authors O´Dowd and Shih (O´Dowd & Shih, 1991). O´Dowd and Shih defined the Q parameter as:

$$Q \equiv \frac{\sigma_{yy} - \left(\sigma_{yy}\right)_{HRR\ or\ T=0}}{\sigma_0} \tag{15}$$

for $\Theta = 0$ and $\frac{r\sigma_0}{J} = 2$

The parameter is equal to zero (Q = 0) under small-scale yielding conditions, but it acquires negative values as the load (and in consequence the strain) grows. Classical single-parameter fracture mechanics assumes that fracture toughness is a material constant. However, the J-Q theory suggests that the critical value of the *J*-integral for a given material depends on the Q parameter – i.e. $J_c = J_c(Q)$ – and that fracture toughness is thus not some single-value quantity, but rather a function that defines the critical values of the *J*-integral and the Q parameter (Shih et al., 1993). Although the relation between critical J-integral values and the Q parameter shows a considerable scatter, the critical value of the *J*-integral tends in general to drop as the Q parameter increases in value.

The theory of single-parameter fracture mechanics assumes that the fracture toughness values obtained on laboratory specimens can be applied to a body. However, two-parameter approaches, such as the J-Q theory, reveal that the specimen must be tested at the same constraint as that of the body with a crack. In other words, the two geometries must have the same Q value at the moment of fracture, so that the corresponding critical values of the *J*-integral, J_{cr}, will be equal to each other. Since J_{cr} values are often scattered to a large extent, we cannot make a clear-cut prediction of this quantity. It is only possible to predict a certain range of plausible J_{cr} values for a given body or structure.

It should also be noted that the J-Q approach is only descriptive, and not predictive. This implies that the Q parameter quantifies the constraint at the crack tip, without providing any indication of the particular influence of the constraint on the fracture toughness. Two-parameter theories cannot be strictly correct as far as their universality is concerned, because they assume two degrees of freedom. Recent research into the influence of the constraint at the crack tip on fracture toughness indicates that geometries with a low constraint can in many cases be judged by a two-parameter theory, and geometries with a high constraint can be judged by a single-parameter theory (Ainsworth & O´Dowd, 1995).

3.2. Plastic constraint factor on yielding

A simple procedure based on the use of the so-called plastic constraint factor on yielding, C, can be applied to determine the fracture conditions in a thin-walled pressure pipeline. The

factor is given by the ratio of the stress needed to obtain plastic macrostrains under constraint conditions to the yield stress at a homogeneous uniaxial state of stress (Gajdoš et al., 2004). The C factor can be expressed by the relation (16)

$$C = \frac{\sigma_1}{\sigma_{HMH}} \tag{16}$$

where σ_{HMH}, the Huber-Mises-Hencky stress, is put equal to the yield stress.

Let us now consider the state of stress at the crack tip in a thick-walled body, where the stress perpendicular to the crack plane, σ_1, and the stress in the direction of the crack, σ_2, are equal, and the stress in the direction of the thickness of the body, σ_3, is governed by the expression $\sigma_3=\nu(\sigma_1+\sigma_2)$. Then, based on the HMH criterion and assumed elastic conditions ($\nu \cong 0.33$), the plastic constraint factor $C \approx 3$. If the stress in the thickness direction, σ_3, falls between $2\nu\sigma_1$ and zero (thin-walled body), the value of the plastic constraint factor will range between $C = 1$ and $C = 3$. This data can be used to assess the fracture conditions in gas pipelines with surface part-through cracks, employing a C-factor which has to be experimentally determined. After the C factor has been determined, the value of $C\sigma_0$ would be used instead of the yield stress σ_0 in relations for calculating the J-integral. The C factor was experimentally investigated at the Institute of Theoretical and Applied Mechanics of the Academy of Sciences of the Czech Republic in the framework of a broader research project on the reliability and operational safety of high pressure gas pipelines. Fracture conditions were investigated on five pipe bodies, made of steels X52, X65 and X70, with cycling-induced cracks. Data on the pipe bodies that were used, the cracks in the walls, and the mechanical and fracture-mechanical material properties of the bodies are given in Table 1.

Material	X 52	X 65	X 65	X 70	X 70
D (mm)	820	820	820	1018	1018
t (mm)	10.2	10.7	10.6	11.7	11.7
c (mm)	50	100	100	127	115
a (mm)	7.0	7.7	7.0	6.7	7.1
a/t	0.686	0.720	0.660	0.573	0.607
a/c	0.14	0.077	0.07	0.053	0.062
p (MPa)	8.05	9.71	9.86	9.86	9.55
$p/p_{0.2}$	1.034	0.750	0.769	0.800	0.775
σ_0 (MPa)	313	496	496	536	536
α	2.40	5.34	5.34	5.92	5.92
n	6.25	8.45	8.45	9.62	9.62
C	2.1	2.4	2.4	2.0	2.07
J_{cr} (N/mm)	487	432	432	439	439
- T/σ_0	0.672	0.575	0.544	0.606	0.611
- Q	0.667	0.591	0.546	0.648	0.651

Table 1. Summary of data on the assessment of the fracture behaviour of model pipe bodies

The rows in the table show the following data (top to bottom): body diameter D, body wall thickness t, half-length of a longitudinal part-through crack c, crack depth a, relative crack depth a/t, aspect ratio a/c of a semi-elliptical crack, fracture pressure p, ratio of fracture pressure p and pressure $p_{0.2}$ corresponding to the hoop stress at the yield stress, yield stress in the circumferential direction of the body σ_0, Ramberg-Osgood constant α, Ramberg-Osgood exponent n, plastic constraint factor C, J-integral critical value J_{cr}, determined as J_m (corresponding to attaining the maximum force at the "force – force point displacement" curve), T-stress to yield stress ratio T/σ_0, and the Q parameter. Values of σ_0, α and n were derived from tensile tests, and the values of J_{cr} were derived from fracture tests run on CT specimens. Fracture pressure values p were read at the moment the ligament under the crack in the pipe body ruptured. Values for the plastic constraint factor on yielding, C, were determined on the basis of the J-integral in such a way that agreement was reached between the predicted and experimentally established fracture parameters for the given crack and fracture toughness of the material. The J-integral value was calculated using the GS method (Gajdoš & Srnec, 1994), on the one hand, and on the basis of the French nuclear code (RCC-MR, 1985), on the other.

It should be noted that in determining the C factor, the critical J-integral value established on CT specimens was considered – namely J_{cr} = 439 N/mm for steel X70, J_{cr} = 432 N/mm for steel X65 and J_{cr} = 487 N/mm for steel X52. It was found by a computational analysis of the CT specimens, employed to construct the R curve, that the Q parameter for these specimens was Q = 0.267. A comparison of this with the Q parameter for pipe bodies ($Q \approx -0.55 \div -0.65$) reveals that the constraint in the CT specimens was much higher. This implies that the real fracture toughness – i.e. the critical value of the J-integral, J_{cr} – was higher in the pipe bodies. The real C factor for a cracked pipe body is lower, so that the *J-a* curve for a pipe body is steeper than the curve for CT specimens with a greater C factor (Gajdoš & Šperl, 2011). Due to this, the J-integral for the axial part-through crack reaches the corresponding higher fracture toughness (for a lower constraint) for the same crack depth as the J-integral with a higher C factor reaches lower fracture toughness (determined on CT specimens). The situation is illustrated in Fig.3.

The normalized T–stress values in Table 1 were obtained using the plane solution – i.e. a solution for a crack of infinite length oriented longitudinally along the pipe. The problem was solved at the Institute of Physics of Materials, Brno, by the finite element method. The solution consisted of two steps: (i) a corresponding FEM network was established and corresponding boundary conditions were formulated for each crack depth, (ii) the magnitudes of the stress intensity factor and the T-stress were calculated for each FEM network by means of the CRACK2D FEM system with hybrid crack elements. The Q parameter values were derived from the $Q - T/\sigma_0$ curves obtained by O´Dowd and Shih (O´Dowd & Shih, 1991), by modified boundary layer analysis for different values of the strain coefficient (Ramberg-Osgood exponent, n). Strictly speaking, the Q parameter values from Table 1 do not correspond accurately to the values for the examined cracks, because the T-stresses were not computed for real semi-elliptical cracks, but for cracks spreading along the entire length of the pipe body ($a/c \approx 0$). Nevertheless, due to the fact that the ratio

of the depth to the surface half-length of the examined cracks (a/c) was close to zero (a/c=0.053÷0.14), we can assume that the differences between the real values of the Q parameter and the values listed in Table 1 will be small.

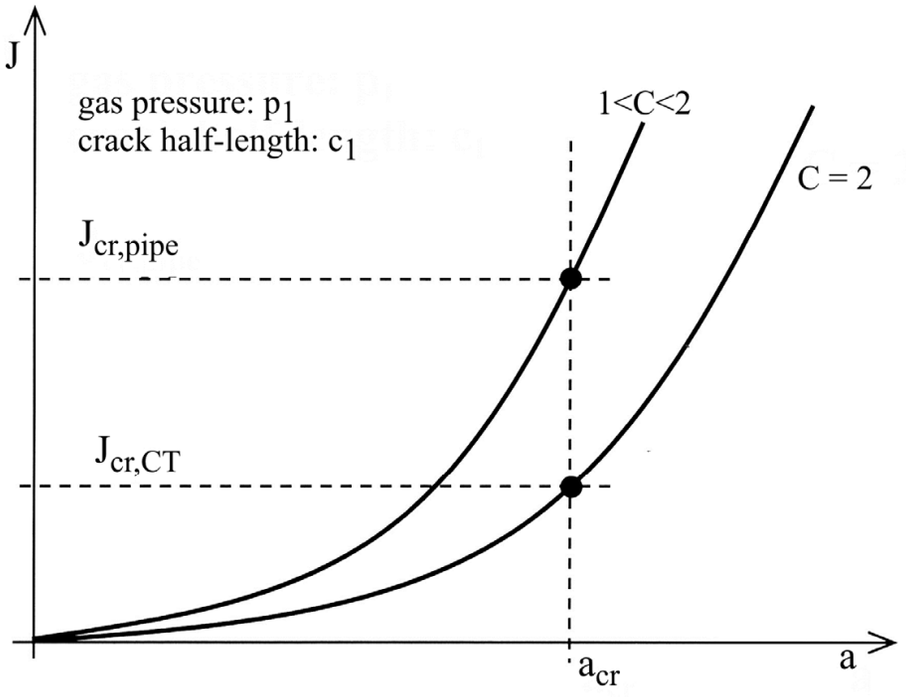


Figure 3. Schematic J-a dependence, (i) for a CT specimen, and (ii) for a pipe with an axial part-through crack

The figures shown in Table 1 provide an idea of the nature of the changes both in the plastic constraint factor, C, and in the Q parameter brought about by changes in the relative crack length, a/t. The diagrams shown in Figs. 4 and 5 can be obtained on the basis of the graphic representation of the pairs $C - a/t$ and $Q - a/t$.

These diagrams clearly show the trends of the changes in the two parameters with a change in the relative crack depth, a/t. It follows that, in the range of relative depths examined here (a/t = 0.57 to 0.72), the plastic constraint factor, C, and the Q parameter are a growing function of the relative crack depth, a/t, the $Q - a/t$ dependence being rather weak. Expressed simply (i.e. linearly), the following relations are involved:

$$C = 2.56\,a/t + 0.53 \tag{17}$$

$$Q = 0.32\,a/t - 0.83 \tag{18}$$

The high scatter of the C and Q values is (i) due to differences in the cross section dimensions of the DN800 and DN1000 pipes and (ii) due to different values of the strain exponent n in the Ramberg-Osgood relation, because the pipes were made of three different materials.

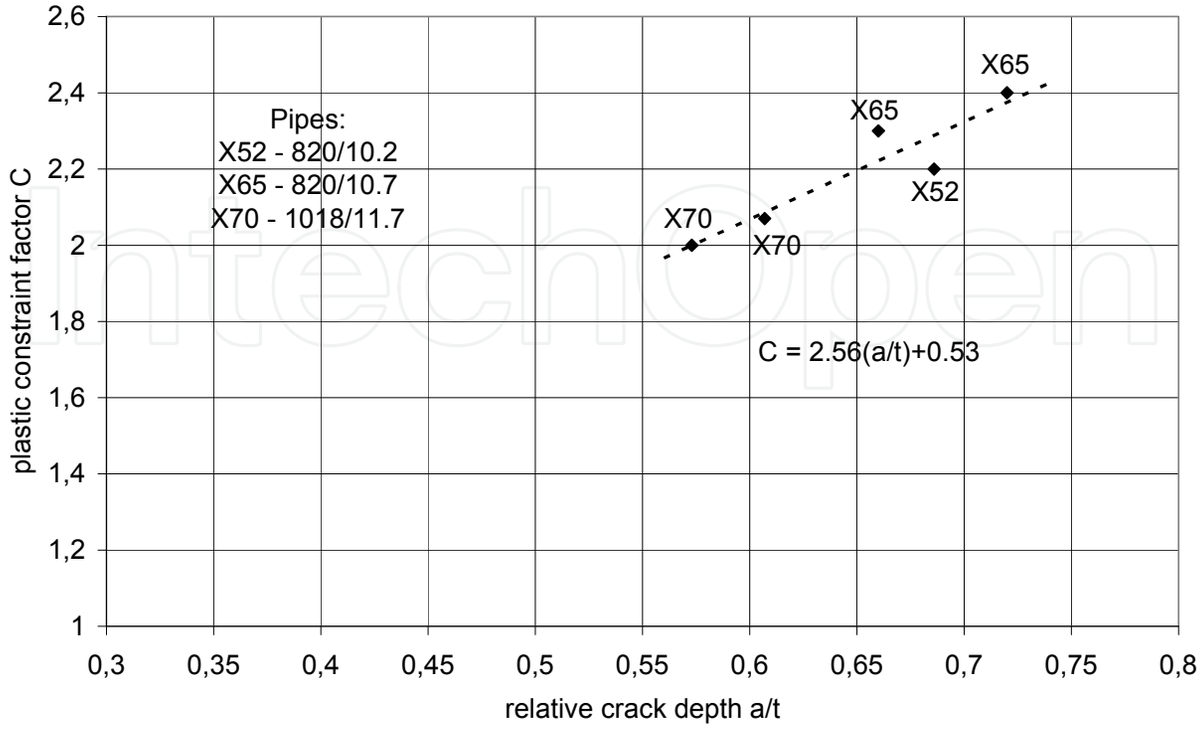


Figure 4. Plastic constraint factor, *C*, as affected by the relative crack depth, *a*/*t*

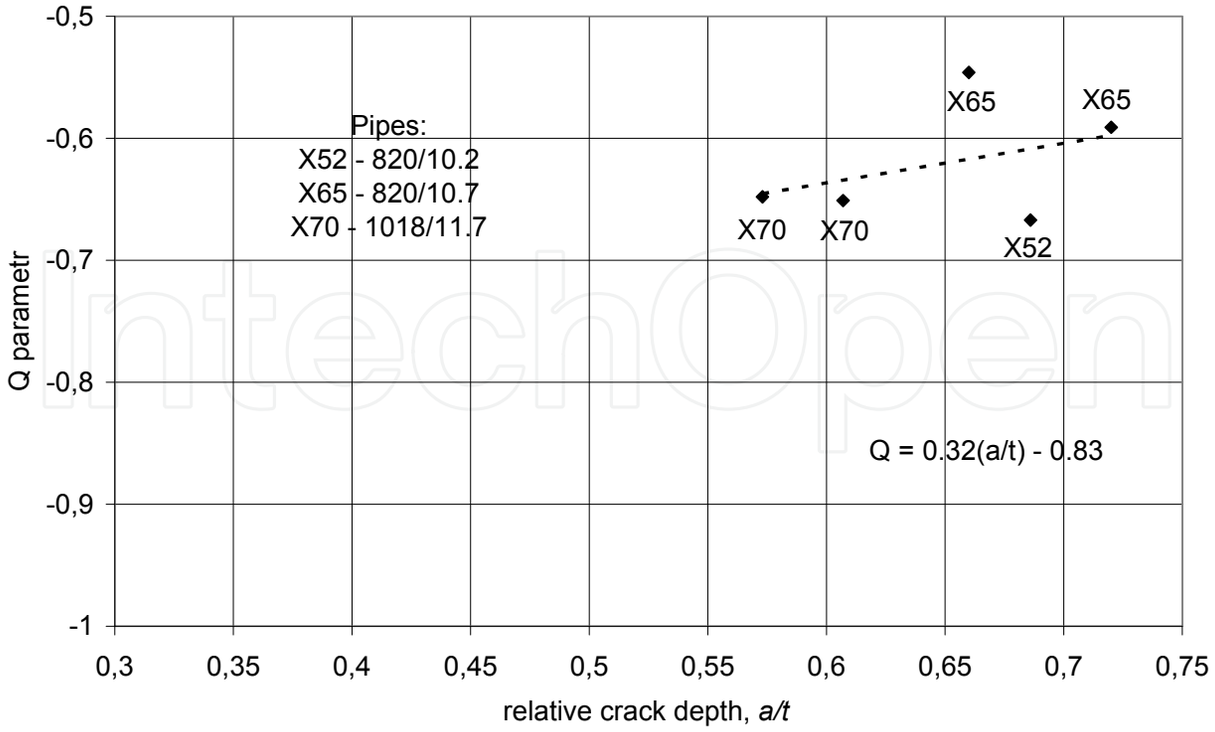


Figure 5. Parameter Q, as affected by the relative crack depth, *a*/*t*

Table 1 lists explicit values of Q and C for all examined cracks in the pipes that were used, and thus a graphic representation of the $C - Q$ relation can be plotted (Fig. 6). In the region where the established values of parameter Q for the examined pipe bodies are found, the $C - Q$ relation can be most simply described by the linear relation:

$$C = 3.4\,Q + 4.3 \tag{19}$$

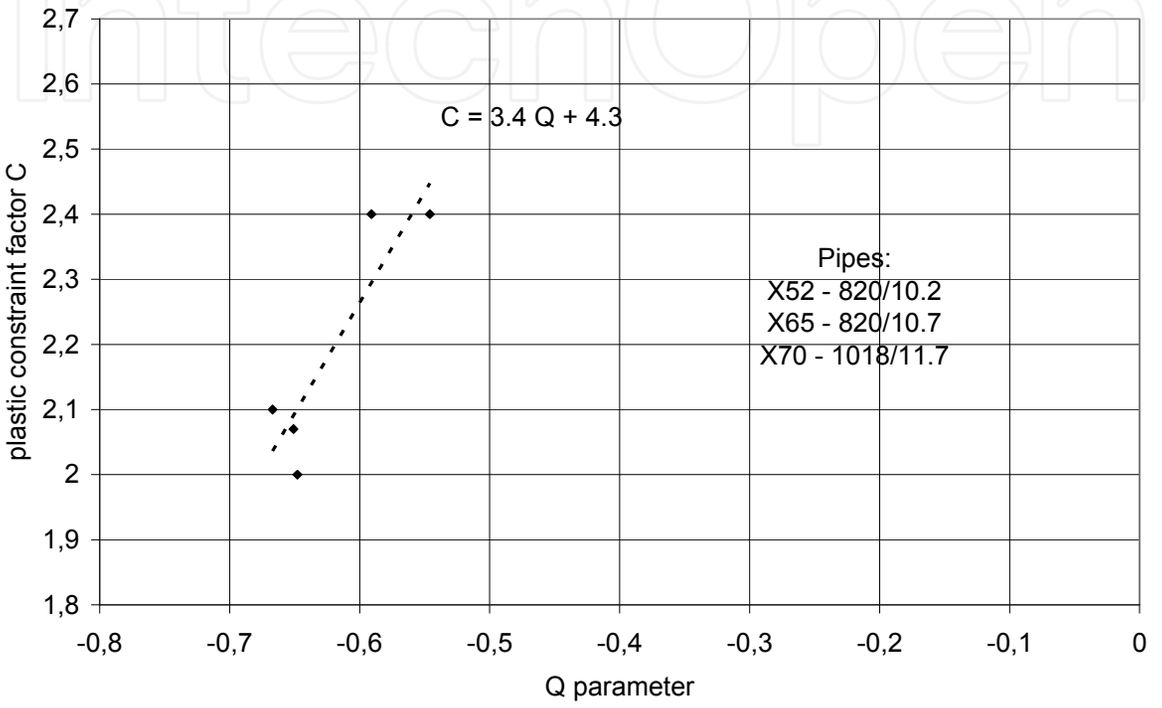


Figure 6. Dependence of the plastic constraint factor, C, on parameter Q

The relation implies that the plastic constraint factor, C, decreases with a decreasing value (increasing negative value) of parameter Q. The observed scatter of the experimental points is mainly due to inaccuracies of the T-stress estimate, which result from the substitution of the real conditions of cracks of certain lengths by the plane solution used in the task (crack along the entire length of the body).

4. Fracture toughness

If we are to evaluate the strength reliability and the remaining life of gas pipelines, we need to get an accurate picture of the properties of the material that the gas pipelines are made of. In the case of gas pipelines operated for different periods of time, we should be aware that the properties of the material of a used pipeline will be different from the initial properties.

In order to pass a qualified judgement on the reliability of a gas pipeline, we should know the true properties that the material displays at the time when the gas pipeline is being examined. The fracture properties can be characterized with sufficient generality by the fracture toughness, determined by quantities J_{in}, $J_{0.2}$, or J_m, where J_{in} is the so-called initiation

magnitude of the J integral for a stable subcritical crack extension; $J_{0.2}$ is the J magnitude corresponding to the real crack extension Δa = 0.2 mm, and J_m is the magnitude of the J integral corresponding to attaining the maximum force at the "force – force point displacement" curve. We should point here to two aspects of fracture toughness that can be encountered when dealing with pressure pipelines. One of them is the effect of pipe band straightening, and the other is the effect of stress corrosion cracks on fracture toughness.

4.1. The effect of straightening

Fracture toughness tests are carried out with fracture mechanical specimens, e.g. single edge notched bend (SENB) specimens or compact tension (CT) specimens. Both types are plane specimens. When investigating the integrity of thin-walled pressure pipelines, we face the problem of ensuring the planeness of the semiproducts for manufacturing the fracture mechanical specimens. The only way is press straightening of pipe bands taken from the pipe that is under investigation. As a consequence of the plastic deformation that the semi-product undergoes during straightening, internal stresses are induced not only in the semi-product but also in the final specimens. Therefore there are still some doubts about the reliability of the fracture toughness characteristics obtained with straightened specimens. In order to verify this matter, Gajdoš and Šperl (Gajdoš & Šperl, 2012) carried out an experimental investigation of fracture toughness, as determined using press straightened CT specimens and curved CT specimens, manufactured directly from a pipe band, i.e. ensuring that their natural curvature and wall thickness were preserved.

The so-called curved CT specimens (see Fig. 7) to some extent simulate the stress conditions in the pipe wall upon loading by internal pressure. In order to apply a circumferential force on these specimens, we used a special testing rig, similar to that developed by Evans (Evans et al., 1995). The rig is shown in Fig. 8.

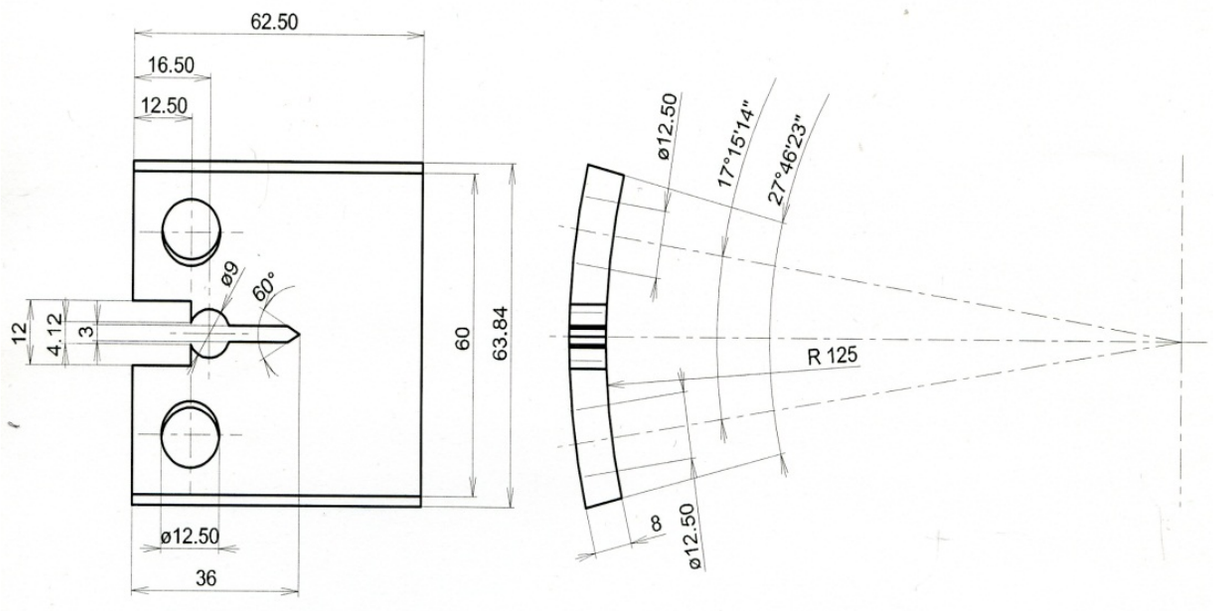


Figure 7. The shape and dimensions of the curved CT specimens

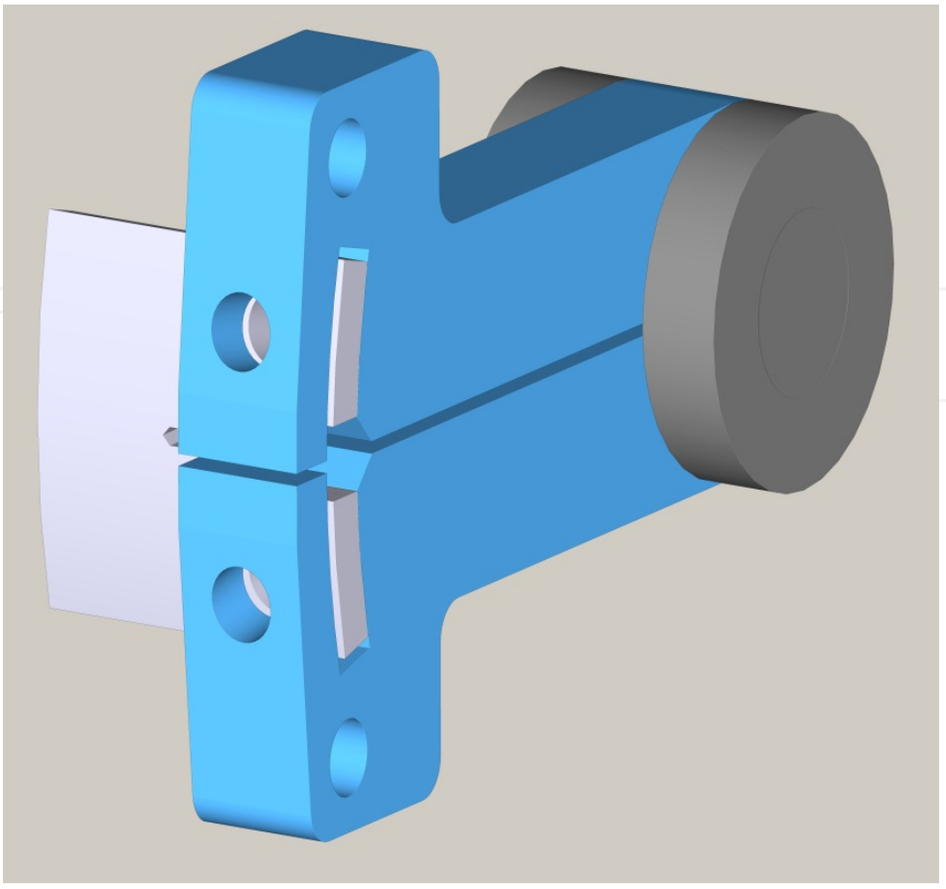


Figure 8. The testing rig for circumferential loading of a curved CT specimen

It is clear that the testing rig is tied with only certain cross – sectional dimensions of a pipe. In the case considered here, the dimensions corresponded to a pipe 266 mm in outside diameter and 8 mm in wall thickness. The material of the pipe was low-C steel CSN 411353. Static tests of the steel provided the following results: $R_{p0.2}$ = 286 MPa; R_m = 426 MPa; A_5 = 31%; Z = 54%. The Ramberg-Osgood constants had the following values: α = 6.23; n = 5.87; σ_0 = 286 MPa.

First, fracture toughness tests were carried out by an ordinary procedure, as specified in the ASTM standard (E 1820-01, 2001), on CT specimens manufactured from a press-straightened band taken from the pipe.

The result in the form of an R-curve is presented in Fig. 9. One point (designated by a triangle) has not been included in the regression analysis because it was outside the valid area of the diagram. The positions of J_{in} and $J_{0.2}$ at the R-curve are clearly defined from the construction of the R-curve, the blunting line and the 0.2 offset line; the position of J_m is also indicated in the diagram, and it represents the mean of six values obtained on specimens where the maximum force was attained in loading the specimens. The R-curve determined by the least-square method is described by a power function (20):

$$J = 327.05\left(\Delta a\right)^{0.6406} \tag{20}$$

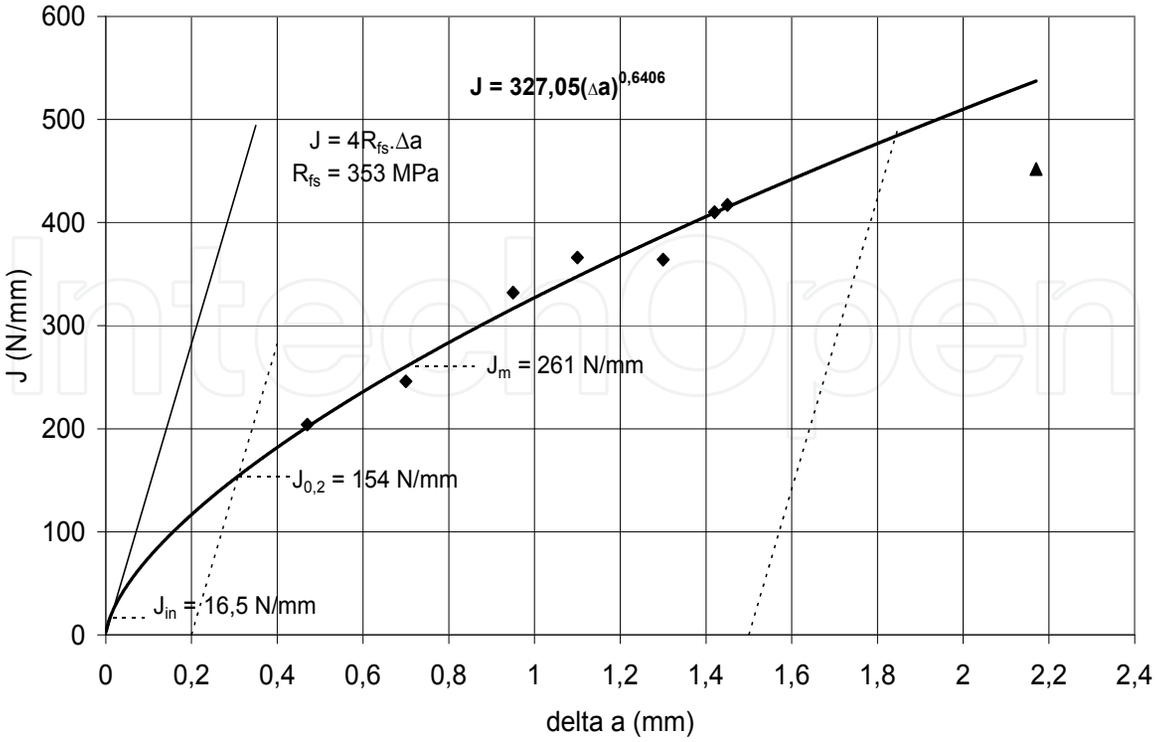


Figure 9. R curve for CT specimens manufactured from a press-straightened semi-product

Eight specimens were used for fracture-mechanical tests of curved CT specimens. Cracks were cycled up at a frequency of 4 Hz, using the testing rig, Fig. 8. The stress state in the inner side of a specimen was bigger than in the outer side, because of the bending moment induced by the out-of-axis action of the vertical component of the tangential force with regard to the intersection of the middle cylindrical area of the specimen with the symmetry plane of the specimen. For this reason, the growth rate of the fatigue crack was higher in the inner side than in the outer side.

This resulted in uneven length of the fatigue crack on the two sides of a specimen after finishing the cycling up. On one half of the specimens, a slant front of the starting notch was therefore made in such a way that the notch was 1 mm deeper on the outer side. By this operation, a much more even front of the fatigue crack was obtained. This is clearly demonstrated in Figs. 10 and 11, which show the fracture surfaces of specimens with a straight front and a slant front of the starting notch. In the two photographs, we can observe areas corresponding to the notch, fatigue, static crack extension and final break after the specimens were cooled down in liquid nitrogen.

On the basis of the finite element analysis and the compliance measurements made by Evans (Evans et al., 1995), it was concluded that the use of standard expressions for determining K factor will not cause error greater than 4% for curved CT specimens. By proceeding in the same way as in standard $J - \Delta a$ testing, an R-curve was obtained for curved CT specimens. It is described by a power function (21), and is presented in Fig. 12.

$$J = 278.21\left(\Delta a\right)^{0.525} \tag{21}$$

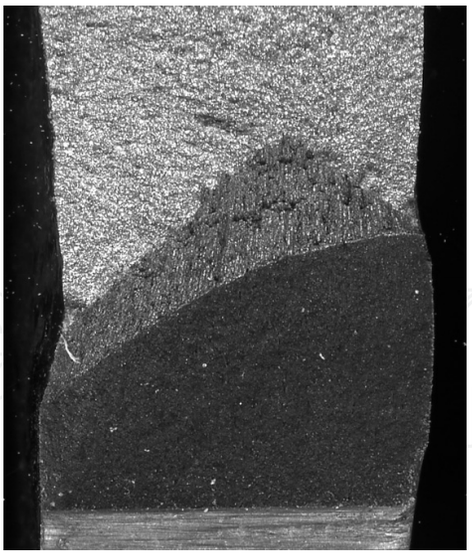


Figure 10. Fracture surface – straight front of the notch



Figure 11. Fracture surface – slant front of the notch

A comparison of the two R-curves shows that the decline of the R-curve obtained with the curved CT specimens is less than the decline of the R-curve obtained with plane, i.e. straightened, CT specimens. The higher decline of the R-curve with the straightened CT specimens is most probably connected with work hardening of a semiproduct during straightening. In the mathematical description of the R-curve of the curved CT specimens, not only the exponent but also the constant is less than for the standard R-curve. This means that the standard R-curve is situated above the R-curve of the curved CT specimens. However, the lower position of the R- curve for the curved CT specimens does not mean significantly lower magnitudes of the fracture toughness characteristics. For example, the J_m value is lower by 1.1%, the $J_{0.2}$ is lower by less than 3%, and the magnitude J_{in} is even higher than the respective characteristics for plane (straightened) CT specimens. In absolute units, the difference is 2.9 N/mm for J_m and 4.6 N/mm for $J_{0.2}$. There is a significant difference in J_{in}, namely 29.7 N/mm in favour of the curved CT specimens.

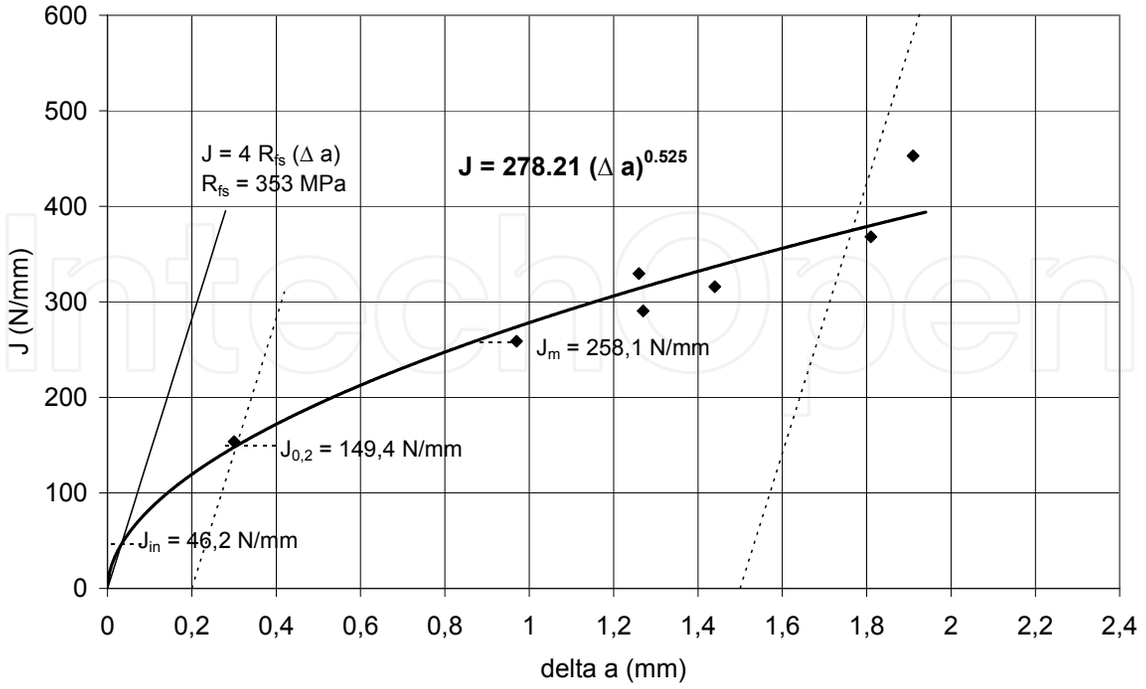


Figure 12. R-curve for curved CT specimens

By accounting the scatter of the results in the form of the J - Δa points, caused both by a natural process of subcritical crack growth and by inaccuracies in determining the J-integral and, in particular, the crack extension during monotonic loading of a specimen, it can be stated with a high level of reliability that the fracture toughness of a pipe material determined on straightened CT specimens is practically the same as the fracture toughness determined on curved CT specimens.

4.2. The effect of stress corrosion

(Gajdoš et al., 2011) investigated the stress corrosion fracture toughness of gas pipeline material, and compared it with fatigue fracture toughness. The material used for the investigation was a low-C steel according to CSN 411353 (equivalent to ASTM A519), containing 0.17% C, 0.035% P, 0.035% S. The test CT specimens were manufactured from a real pipe section cut out from a DN 150 gas pipeline 4.5 mm in wall thickness while it was being repaired after 20 years of operation. Before the CT specimens were manufactured, the pipe section was press straightened. Owing to the small thickness of the specimens (a low constraint), the fracture toughness values cannot be qualified to represent the real fracture toughness values. However, they can be used as a comparative measure of fracture toughness, thus enabling quantification of the effect of stress corrosion cracks on the apparent fracture toughness.

The CT specimens were first cyclically loaded by a routine procedure used in determining fracture toughness; the only difference was that the cycling was stopped when the growth of the fatigue crack reached approximately the magnitude $\Delta a_{FA} \approx 1.5$ mm. After that, the CT

specimens were put into the stress-corrosion (SC) crack generator with an acidic solution according to the NACE Standard (NACE Standard TM0177, 2005). This solution consisted of 50 g NaCl (sodium chloride) + 5 g CH_3COOH (acetic acid) + 945 g H_2O, and during the generating process it was bubbled by H_2S (hydrogen sulphide). A constant force F of 3 kN was applied to the specimens. The corresponding level of the nominal stress (tension and bending) at the fatigue crack tip exceeded the yield stress $R_{p0.2}$ by about 25%. The crack length increment due to stress-corrosion Δa_{SC} was determined with the help of the relations for elastic crack-edge displacements at CT specimens. In total, three groups of CT specimens were prepared. The first group (A) was the reference group; the specimens from this group contained only the fatigue crack. The second group of CT specimens (B) contained specimens that were left freely in air at the indoor temperature for two weeks after being removed from the SC crack generator, and were then subjected to fracture toughness tests. The specimens from the third group (C) were tested immediately after they had been removed from the SC crack generator (the time difference between testing the first specimen and the last specimen being approximately 20 minutes).

The results confirmed that the fracture resistance of a component (given by the apparent fracture toughness) depends not only on the material of the component and on the crack tip constraint (the thickness of the wall of the component) but also on the origin of the crack (fatigue, stress corrosion), and thus on the corresponding crack growth mechanism. In contradiction with the opinion that low-C steels are not susceptible to stress corrosion cracking our results showed that under conditions specified in (NACE Standard TM0177, 2005) stress corrosion cracks can also be generated from fatigue cracks in low-C steels such as CSN 411353. Unlike a fatigue crack, the occurrence of a stress-corrosion crack in a component means a significant decrease in the fracture toughness characteristics while the crack is exposed to stress corrosion conditions, and a partial "recovery" of the fracture toughness when the stress corrosion conditions are removed. The results for all three groups of specimens are summarized in Fig. 13.

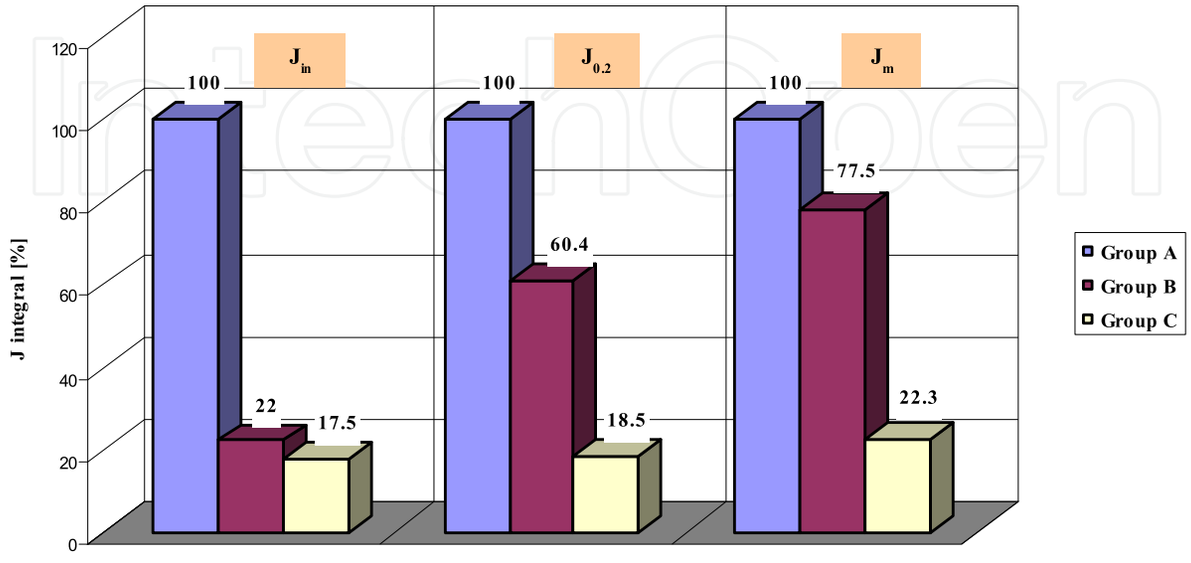


Figure 13. A bar chart of the J integral values for specimens of groups A, B and C

As this figure shows, the stress corrosion fracture toughness characteristics for the low-C steel CSN 411353 were lower than the fatigue fracture toughness characteristics by a factor ranging between 4.5 (J_m value) and 5.7 (J_{in} value). However, a two-week recovery period made it possible to recover their fracture properties to some extent, namely the J-integral J_m to almost 80%, the J-integral $J_{0.2}$ to about 60%, and the J-integral J_{in} to about 22% of the fatigue crack J-integral values. It follows from here that in evaluating the reliability of gas pipelines it is always necessary to examine the character of the cracks in the pipe wall, and in the case of stress corrosion cracks to take into account that the fracture toughness can be drastically lower than the values determined on specimens with cracks of fatigue origin.

5. Burst tests

An experimental verification of the fracture conditions of gas pipelines can be made most accurately on a test pipe body cut out of the gas pipeline to be examined. When deciding on the length of the test pipe body, we should bear in mind that the working length of the body (characterized by the absence of stress effects from welded-on bottoms) will be shorter by $2 \times 2.5\sqrt{(Rt)} \approx 3.5\sqrt{(Dt)}$. It is usually sufficient for the distance between the welds of dished bottoms to be at least $3.5D$. This length permits a number of starting cuts to be placed axially along the length of the body. The cuts are made to initiate crack growth when the body is subsequently pressurized by a fluctuating pressure. The cuts can be made in several ways, one of which uses a thin grinding wheel. The smallest real functional thickness of such a wheel is about 1.2 mm, and the corresponding width of the cuts made with it is approximately 1.5 mm. Depending on the type of pipes of which gas pipelines are built (seamless, spirally welded, longitudinally welded), the starting cuts can be provided in the base material, in the transition region or in the weld metal, their orientation being axial, circumferential or along the spiral weld.

5.1. Preparation of test pipe bodies

It is appropriate to relate the surface length of the cuts to the wall thickness of the pipe body. Testing the body for the danger posed by so-called long cracks should be carried out with crack lengths not exceeding twenty times the wall thickness of the pipe body. The situation with the depth of the starting cuts is different. The depth of an initiated fatigue crack must be at least 0.5 mm along the whole perimeter of the cut tip, so that the cut with the initiated crack at its tip can be considered as a crack after the pipe body has been subjected to cycling. This value follows from the work done by Smith and Miller (Smith & Miller, 1977). If such a crack a_t in size finds itself in a notch root defined by depth a_v and radius of the roundness ρ (see Fig. 14), this configuration can be regarded as a surface crack a_e in depth, where

$$\begin{aligned} a_e &= \left(1 + 7.69\sqrt{\frac{a_v}{\rho}}\right) a_t \quad for \quad a_t < 0.13\sqrt{a_v \rho} \\ a_e &= a_v + a_t \quad for \quad a_t \geq 0.13\sqrt{a_v \rho} \end{aligned} \tag{22}$$

It is evident that for $a_t \geq 0.13\sqrt{a_v \rho}$, a cut with a crack along the perimeter of the cut tip can be taken for a crack with a depth of $a_v + a_t$. For the cut width 2ρ = 1.5–2.0 mm and the notch depth a_v = 6–10 mm (in relation to the wall thickness), we find that the fatigue increment of the size of the initiated crack, a_t, should be greater than about 0.5 mm.

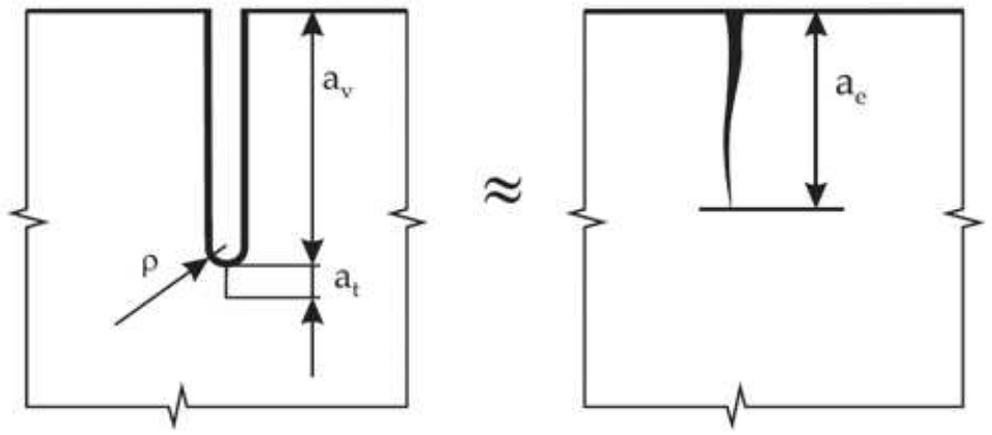


Figure 14. Substitution of a notch with a crack by the equivalent crack

As described in paragraph 3.2, three test pipe bodies, made of X52, X65 and X70 steels, were provided with working slits and so-called check slits, which were of the same surface length as the working slits but their depth was greater. These check slits functioned as a safety measure to prevent cracks that developed at the working slits from penetrating through the pipe wall. For illustration, a DN1000 test pipe body with a working length of 3.5 m is shown in Fig. 15. The check slits are denoted in Fig. 15 by a supplementary letter K. The material of the test pipe body is a thermo-mechanically treated steel X70 according to API specification. The pipe is spirally welded, the weld being inclined at an angle of $\varphi = 62°$ to the pipe axis. It is provided with starting cuts oriented either axially or in the direction of the strip axis (i.e. in the direction of the spiral) and then along or inside the spiral weld. The cuts differ in length ($2c$ = 115 mm or 230mm) and in depth (a = 5, 6.5, 7, and 7.5 mm). We are particularly interested in axial (longitudinal) slits situated aside welds, because these are sites where axial cracks will be formed in the basic material of the pipe.

Efforts were made in the fracture tests to keep the circumferential fracture stress below the yield stress, because the operating stress in gas pipelines is virtually around one half of the yield stress (and does not exceed two-thirds of the yield stress even in intrastate high-pressure gas transmission pipelines). Calculations reveal that in order to comply with this, the depth of the axial semi-elliptical cracks should be greater than one half of the wall thickness. Oblique cracks should be even deeper, as the normal stress component opening these cracks is smaller. If the crack depth is to have a certain magnitude before the fracture test is begun, the depth of the starting slit should be smaller than this magnitude by the fatigue extension of the crack along the perimeter of the slit tip. At the same time, we should bear in mind that the greater the fatigue extension of the crack, the better the agreement with a real crack.

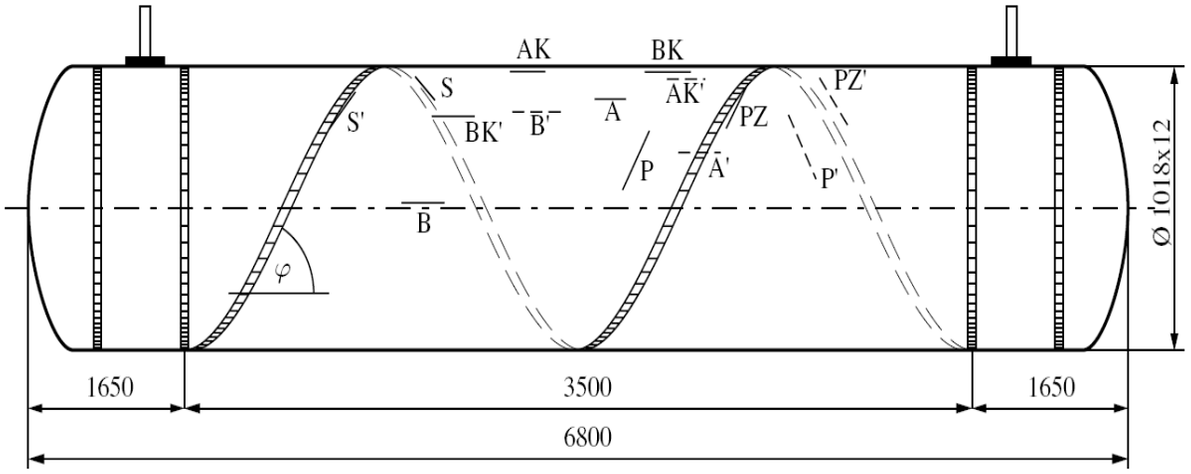


Figure 15. Test pipe body with the starting cuts marked

5.2. Prediction of fracture parameters

After the starting slits were made, the test pipes were subjected to water pressure cycling to produce fatigue cracks in the tips of the starting slits. The cycling was carried out in a pressurizing system, which included a high-pressure water pump, a collecting tank, a regulator designed to control the amount of water that was supplied and, consequently, the rate at which the pressure is increased in the pipe section. This was effected by opening by-pass valves.

In cycling the cracks, the water pressure fluctuated between p_{min} = 1.5 MPa and p_{max} = 5.3 MPa, and the number of pressure cycles was between 3 000 and 4 000. The period of a cycle was approximately 150 seconds. The cycling continued until a crack initiated in one of the check slits became a through crack. This moment was easy to detect, because it was accompanied by a water leak. By choosing an appropriate difference between the depths of the working slits and the check slits it was possible to obtain a working crack depth (= starting slit depth + fatigue crack extension) of approximately the required size. To run a test for a fracture, however, it was necessary to remove the check slit which had penetrated through the wall of the test pipe from the body shell and to repair the shell, e.g. by welding a patch in it.

After removing the check slit with a crack which penetrated through the wall, and repairing the shell of the test pipe, the pipe was loaded by increasing the water pressure to burst. The test procedure, which was common for all test pipes, will now be briefly described for the DN1000 pipe shown in Fig. 15. As the figure suggests, slits A, A′, B and B′ were oriented along the axis of the pipe. The nominal length of notches B, B′ was twice as long as notches A, A′, but notches B, B′ were shallower. As was mentioned above, the cracks at the slit tips were extended by fluctuating water pressure, and this proceeded until the cracks from the check slits (BK, BK′) grew through the wall and a water leak developed. Then the damaged parts of the shell were cut out, patches were welded in their place, and the test pipe was monotonically

loaded to fracture at the location of crack B or B′. The burst of the test pipe at crack B is shown in Figs. 16 and 17 (as a detail). A part of the fracture surface is shown in Fig. 18.

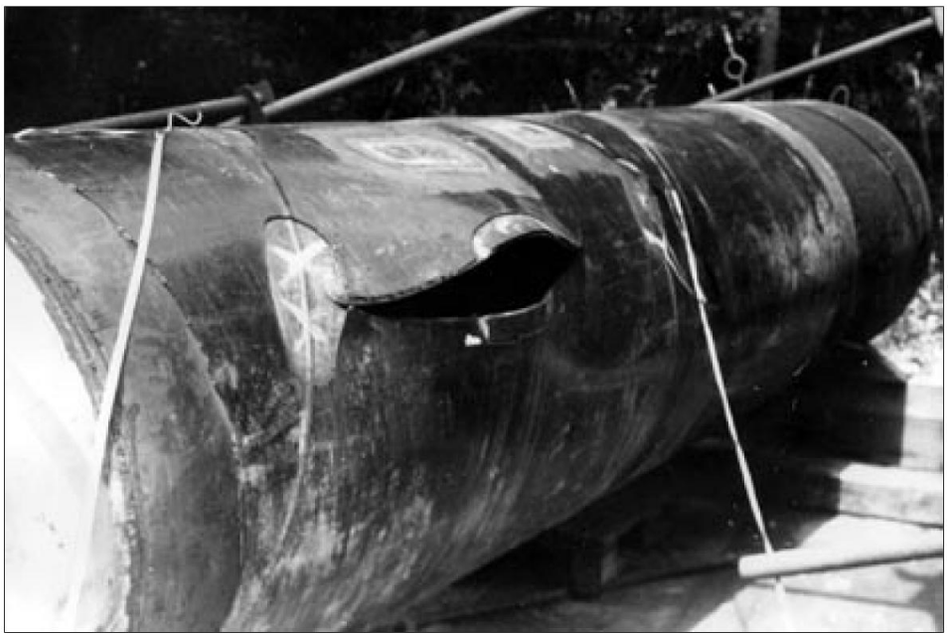


Figure 16. Burst initiated on slit B with a fatigue crack



Figure 17. Burst initiated on slit B – a detail

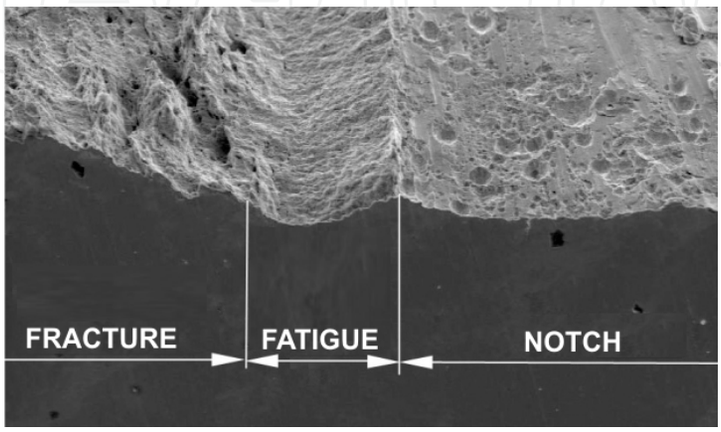


Figure 18. A part of the fracture surface of crack B (fatigue region ~ 2.4 mm)

Evidently, at the instant of fracture the crack spread not only through the remaining ligament, but also lengthwise. After removing the part of the pipe shell with crack B, a patch was welded in and the second burst test followed. Table 2 extracts from Table 1 the numerical values of the geometrical parameters, the J-integral fracture values, the Ramberg-Osgood constants, the fracture pressure and the fracture depth for cracks B and B′, respectively.

Characteristics	Crack B	Crack B′
CRACK DIMENSIONS		
half-length, c (mm)	115	127
depth in fracture, a_f (mm)	7.1	6.7
RAMBERG-OSGOOD PARAMETERS		
α / n /σ_0 (MPa)	5.92 / 9.62 /536	5.92 / 9.62 /536
FRACTURE TOUGHNESS		
$J_{cr} = J_m$ (N/mm)	439	439
FRACTURE PRESSURE		
p_f (MPa)	9.55	9.86

Table 2. Some characteristics referring to crack B and crack B′

It should be noted that Table 2 includes the Ramberg-Osgood constants for the circumferential direction of the test pipe, with the crack oriented axially in the pipe. This is because the stress-strain properties perpendicular to the crack plane are crucial in determining the J-integral for an axial crack. The stress-strain dependence in the circumferential direction should therefore be taken into account where an axial orientation of the crack is concerned. The most important fracture test results from the viewpoint of the fracture conditions are the magnitudes of the fracture pressure, p_f, and the fracture depth, a_f, for a given crack length $2c$. It follows from Table 2 that p_f = 9.55 MPa and a_f = 7.1 mm for crack B, and p_f = 9.86 MPa and a_f = 6.7 mm for crack B′. These values are also shown in the last two columns of Table 1.

Now let us predict the fracture conditions according to engineering approaches, and compare the prediction results with the real fracture parameter values (pressure, crack depth). The procedure for verifying the engineering methods for the predictions involves determining either the fracture stress for a given (fracture) crack depth, or the fracture crack depth for a given (fracture) pressure. To illustrate this, we select the latter case – i.e. determining the fracture depth of a crack for a given (fracture) pressure. Fig. 19 shows the J-integral vs. crack B depth dependences, as determined by the FC and GS predictions for the fracture hoop stress given by the measured fracture pressure. When using equations (9), (10), and (12) to determine J-integrals, the following parameters were used for the calculation: D = 1018 mm; t = 11.7 mm ; $p = p_f$ = 9.55 MPa; c = 115 mm; α = 5.92; n = 9.62; σ_0 = 2.07×536 = 1110 MPa (i.e. C = 2.07). Fig. 20 shows similar dependences for crack B′.

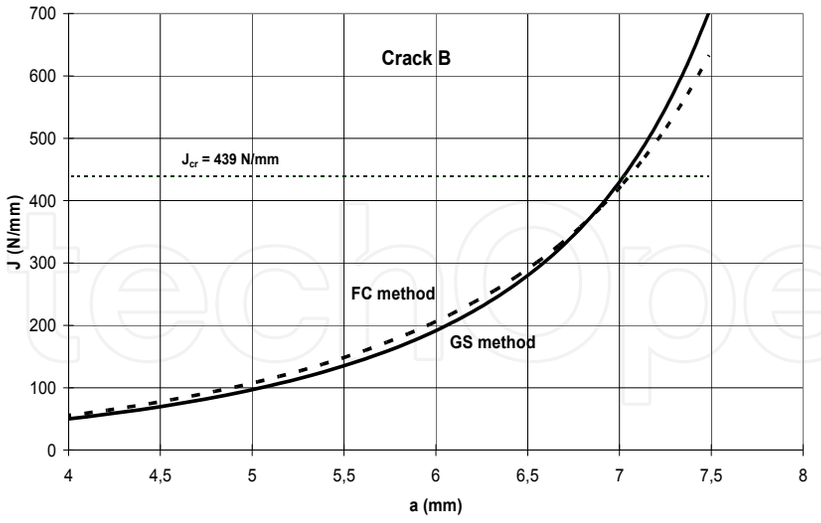


Figure 19. Prediction of the fracture depth for crack B ($p = p_f = 9.55$ MPa and C = 2.07)

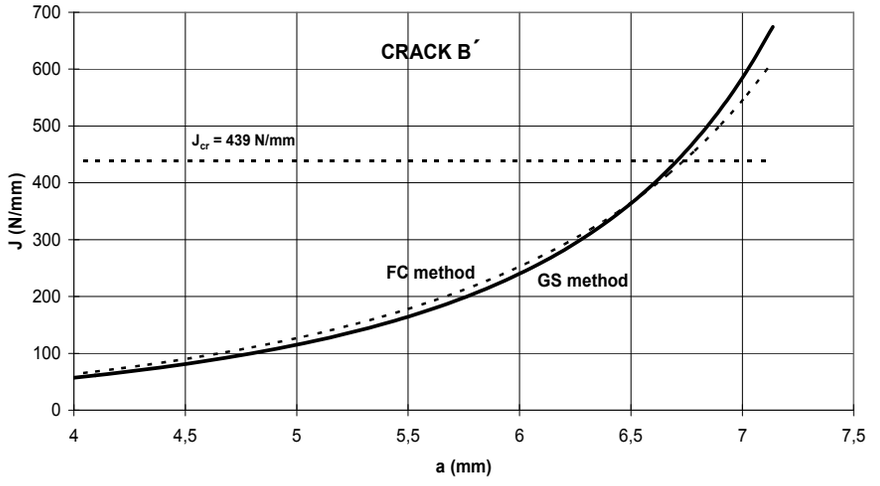


Figure 20. Prediction of the fracture depth for crack B´ ($p = p_f = 9.86$ MPa and C = 2.0)

The same computational parameters as those employed in the case of crack B were used in the equations to determine the J-integral according to the FC and GS methods, with the exception of the fracture pressure (p_f = 9.86 MPa), the crack half-length (c = 127 mm) and factor C (C = 2.0). As is evident from Fig. 19, the intersection of the straight line $J = J_{cr}$ = 439 N/mm with the two $J - a$ curves gives the value $a_{cr} \approx 7.05$ mm, which is well consistent with crack depth B a_{cr} = 7.1 mm, established experimentally. Similarly, the intersection of the straight line $J = J_{cr}$ = 439 N/mm with the $J–a$ curves according to the FC and GS procedures in Fig. 20 shows the fracture crack depth a_{cr} to be virtually identical to the experimentally found fracture depth a_f = 6.7 mm. For other test pipes, namely DIA 820/10.7, made of X65 steel, and DIA 820/10.2, made of X52 steel, various magnitudes of the plastic constraint factor C were obtained to achieve good agreement of the geometric parameters at fracture with the experimental parameters. They are illustrated in Fig. 4. The conclusion can thus be

drawn that very good agreement of the fracture parameter values predicted by the FC and GS engineering approaches with the values found experimentally can be achieved when using the plastic constraint factor on yielding, C, at the level $C = 2$. If a higher value of the C factor provides more precise results, the use of the value C = 2 will yield a conservative result.

6. Conclusion

A specific fracture-mechanics-based procedure for assessing the integrity of pressurized thin-walled cylindrical shells made from steels includes a theoretical treatment for cracks in pipes. On the basis of both experimental work and a fracture-mechanical evaluation of experimental results, an engineering method has been worked out for assessing the geometrical parameters of critical axial crack-like defects in a high-pressure gas pipeline wall for a given internal pressure of a gas. The method makes use of simple approximate expressions for determining fracture parameters K, J, and it accommodates the crack tip constraint effects by means of the so-called plastic constraint factor on yielding. Involving this in the fracture analysis leads to multiplication of the uniaxial yield stress by this factor in the expression for determining the J-integral. Two independent approximate equations for determining the J-integral provided very close assessments of the critical geometrical dimensions of part-through axial cracks. With the use of the crack assessment method, the critical gas pressure in a pipeline can also be determined for a given crack geometry.

The fracture toughness with which the J-integral is compared in fracture analysis is determined using fracture mechanics specimens (e.g. CT, SENB and others). Experiments made on press-straightened CT specimens and on curved CT specimens with a natural curvature, made from pipe 266/8 mm of low-C steel CSN 411353, showed that straightening a pipe band prior to the machining of CT specimens had a practically negligible effect on the fracture toughness characteristics ($J_{0.2}$, J_m). However, experiments with fracture toughness testing of specimens with stress corrosion cracks, formed by the hydrogen mechanism, showed a dramatic reduction of all fracture toughness characteristics in comparison with fracture toughness determined on specimens with fatigue cracks, e.g. the quantities J_{in}, $J_{0.2}$ and J_m dropped to 17.5%, 18.5%, and 22.3%, respectively. A partial "recovery" of fracture toughness characteristics was observed when the stress corrosion conditions were removed.

Author details

Ľubomír Gajdoš and Martin Šperl
Institute of Theoretical and Applied Mechanics, Academy of Sciences of the Czech Republic, Czech Republic

Acknowledgement

Financial support from Research Plan AV0Z 20710524 and from grant-funded projects GACR P105/10/2052 and P105/10/P555 are highly appreciated.

7. References

Ainsworth, R. A. & O´Dowd, N. P. (1995). Constraint in the Failure Assessment Diagram Approach for Fracture Assessment. *Transactions ASME – Journal of Pressure Vessel Technology*, Vol.117, pp. 260-267

ASTM Standard E 1820-01 (2001). *Standard Test Method for Measurement of Fracture Toughness*, 2001

Erdogan, F. & Kibler, J. J. (1969). Cylindrical and Spherical Shells with Cracks. *International Journal of Fracture Mechanics,* Vol.5, No.3, pp. 229-237

Erdogan, F.; Delale, F. & Owczarek, J. A. (1977). Crack Propagation and Arrest in Pressurized Containers. *Journal of Pressure Vessel Technology,* Vol.99, (February 1977), pp. 90-99

Evans, J. T., Kotsikos, G. & Robey, R. F. (1995). A method for Fracture Toughness Testing Cylinder Material. *Engineering Fracture Mechanics,* Vol.50, No.2, pp. 295-300

Folias, E. S. (1969). On the Effect of Initial Curvature on Cracked Flat Sheets. *International Journal of Fracture Mechanics,* Vol.5, No.4, pp. 327-346

Folias, E. S. (1970). On the Theory of Fracture of Curved Sheets. *Engineering Fracture Mechanics,* Vol.2, No.2, pp. 151-164

Gajdoš, Ľ. & Srnec, M. (1994). An Approximate Method for J Integral Determination. *Acta Technica CSAV*, Vol.39, No.2, pp. 151-171

Gajdoš Ľubomír et al. (2004). *Structural Integrity of Pressure Pipelines.* Transgas, 80-86616-03-7, Prague, Czech Republic

Gajdoš, Ľ. & Šperl, M. (2011). Application of a Fracture-Mechanics Approach to Gas Pipelines. *Proceedings of World Academy of Science, Engineering and Technology*. Vol.73, January 2011, pp. 480 - 487

Gajdoš, Ľ., Šperl, M. & Siegl, J. (2011). Apparent Fracture Toughness of Low-Carbon Steel CSN 411353 as Related to Stress Corrosion Cracks. *Materials and Design*, Vol.32, No.8-9, pp. 4348-4353

Gajdoš, Ľ. & Šperl, M. (2012). The Effect of Straightening a Curved Body on Its Fracture Properties (in Czech). In: *Proceedings of the 21st Colloquium "Safety and Reliability of Gas Pipelines"*, Prague, 2012

Hutchinson, J. W. (1968). Singular Behaviour at the End of a Tensile Crack Tip in a Hardening Material. *Journal of the Mechanics and Physics of Solids*, Vol.16, pp. 13-31

Milne, I.; Ainsworth, R. A.; Dowling, A. R. & Stewart, A. T. (1986). *Assessment of the Integrity of Structures Containing Defects*. CEGB Report No. R/H/R6 – Rev.3, Central Electricity Generating Board, London, U.K., (1986)

NACE Standard TM0177 (2005). *Laboratory Testing of Metals for Resistance to Sulfide Stress Cracking and Stress Corrosion Cracking in H_2S Environments.* Item No. 21212, 2005

Newman, J. C. (1973). Fracture Analysis of Surface and Through-Cracked Sheets and Plates. *Engineering Fracture Mechanics*, Vol.5, No.3, pp. 667-689

O´Dowd, N. P. & Shih, C. F. (1991). Family of Crack-Tip Fields Characterized by a Triaxiality Parameter – I. Structure of Fields. *Journal of the Mechanics and Physics of Solids,* Vol.39, pp. 898-1015

RCC – MR (1985). *Design and Construction Rules for Mechanical Components of FBR Nuclear Island*. First Edition (AFCEN–3-5 Av. De Friedeland Paris 8), (1985)

Rice, J. R. & Rosengren G. F. (1968). Plane Strain Deformation near a Crack Tip in a Power-Law Hardening Material. *Journal of the Mechanics and Physics of Solids*, Vol.16, pp. 1-12

Scott, P. M. & Thorpe, T. W. (1981). A Critical Review of Crack Tip Stress Intensity Factors for Semi – Elliptical Cracks. *Fatigue of Engineering Materials and Structures*, Vol.4, No.4, (1981), pp. 291 – 309

Shah, R. C. & Kobayashi, A. S. (1973). Stress Intensity Factors for an Elliptical Crack Approaching the Surface of a Semi – Infinite Solid. *International Journal of Fracture*, Vol. 9, (1973), pp. 133-146

Shih, C. F.; O´Dowd, N. P. & Kirk, M. T. (1993). A Framework for Quantifying Crack Tip Constraint. In: *Constraint Effects in Fracture*. ASTM STP 1171, American Society for Testing and Materials, Philadelphia, pp. 2-20

Smith, R. A. & Miller, K. J. (1977). Fatigue Cracks at Notches. *International Journal of Mechanical Sciences*, Vol.19, pp. 11-22

IntechOpen